Electronic Supplementary Material (ESI) for Green Chemistry.

Supporting Information

Address the Challenge of Fabricating High Content of Regenerated Cellulose/Nanomaterial Composite: Magical Effect of Urea

Kai Wu,*[a b] Dingyao Liu,[a b] Feng Gong [c], Chuxin Lei [b] and Qiang Fu *[b]

[a] Key Laboratory for Soft Chemistry and Functional Materials of Ministry of Education, Department of Polymer Science and Engineering, School of Chemical Engineering, Nanjing University of Science and Technology, Nanjing 210094, PR China.

[b] College of Polymer Science and Engineering, State Key Laboratory of Polymer Materials Engineering, Sichuan University, Chengdu 610065, PR China.

[c] School of Energy and Environment, Southeast University, Nanjing 210094, PR China.

Corresponding author

E-mail: kaiwu@njust.edu.cn (K. Wu);

E-mail: qiangfu@scu.edu.cn (Q. Fu), Tel./Fax: +86 28 8546 1795;

1. Experimental Section

Materials: The cellulose raw material (cotton linter pulp) is supplied by Jilin Chemical Fiber Group Ltd., China. Hexagonal boron nitride (h-BN) with the lateral size of 30 μm was obtained from Shengyi Technology Ltd., China, and it was further exfoliated to be single-layer BNNSs (Figure S1a-c) according to our previous method.[1] MWCNT (NC7000), length of 1.5 μm and diameter of 9.5 nm (Figure S1e), were purchased from Nanocyl S.A, Belgium. GNPs (XTG-P-0762, Figure S1f) were provided by Deyang Carbonene Science Co. Ltd., China. Urea, $LiOH \cdot H_2O$, phytic acid, Na_2SO_4, LiCl and epichlorohydrin were purchased from Aladdin Reagent Limited Corporation in China and used without any further purifications.

Preparation of cellulose/nanomaterial inks: As shown in Figure 1, typical amount of nanomaterial, for example BNNSs, MWCNT or GNPs, was firstly ball-milled at 500 rpm with urea (7.2 g) in 36.96 g H_2O for 30 min. And cellulose was dissolved in an alkali/urea aqueous solution. Typically, 8 g $LiOH \bullet H_2O$, 15 g urea and 77 g H_2O were stirred together and pre-cooled to −12 °C. Then, 950 rpm intense stirring was applied to dissolve cellulose pulp, as suitable amount of cellulose raw material was slowly added until cellulose solvent became totally transparent. Then, above transparent cellulose solution, nanomaterial slurry and supplementary $LiOH \bullet H_2O$ were mixed together, followed with a 3 min defoaming process by a conditioning mixer (AR-100) to obtain the stable cellulose/nanomaterial ink. Noted that the filler concentration of the ink is defined as m_{filler}/V_{ink}, where m_{filler} is the added filler weight, and V_{ink}

is the final volume of the composite ink, which is almost similar to the volume of H_2O in the whole system.

Preparation of 1D RC/BNNSs multi-filaments: Continuous wet-spinning method was utilized to produce RC and RC/BNNSs multi-filaments through a pilot-scale spinning machine (made by Chengdu Science and Technology Co., Ltd). In a typical procedure, viscous cellulose or cellulose/BNNSs ink (4.2 g cellulose in 110.5 g ink, cellulose/BNNSs=40 wt/60 wt) was slowly squeezed out from the spinneret cylinder into a coagulation bath (15 wt % phytic acid/5 wt % Na_2SO_4). And partially solidified RC or RC/BNNSs multi-filaments were collected by a Nelson-type roller. Afterwards, these multi-filaments were washed by 30 °C distilled water to remove any residual salts and acids, followed by forced air dried at 60 °C for 2 h for further use and characterizations. Noted that the filler concentration of the RC composite materials is defined as $m_{filler}/m_{composite}$, where m_{filler} is the added filler weight, and $m_{composite}$ is the sum value of added filler weight and added cellulose weight.

Preparation of 2D RC/MWCNT film: Firstly, highly concentrated cellulose/MWCNT ink (3 g cellulose in 106 g ink, cellulose/MWCNT=50 wt/50 wt) was slit-coated on a glass plate. Then, it was immersed in a coagulation bath (15 wt % phytic acid/5 wt % LiCl) for 5 min to promote the regeneration of RC/MWCNT film. Finally, solidified RC/MWCNT gel-like film were washed by 30 °C distilled water to remove any residual salts and acids, followed by forced air dried at 60 °C for 2 h for further use and characterizations.

Preparation of 3D porous RC/GNPs nanocomposites: Above highly concentrated cellulose/GNPs ink (3 g cellulose in 106 g ink, cellulose/GNPs=50 wt/50 wt) was casted into a copper mold and kept at 60 ^{o}C for 24 h for physical gelation. Then, obtained cellulose/GNPs hydrogel was washed by 60 ^{o}C water to lead the regeneration of RC and removal of urea and LiOH. Finally, above RC/GNPs hydrogel was frozen by liquid N_2 and then freeze-dried for 72 h to prepare the porous RC/GNPs nanocomposites.

Characterization: The microscopic morphology was characterized by field-emission scanning electron microscope (SEM, JSM-7500F, Jeol), transmission electron microscopy (TEM, JEF-2100F, Jeol, Japan) and atomic force microscopy (AFM, 359 Marin Keys Bivd, Suite 20, USA). Rheological property of cellulose, cellulose/BNNSs, cellulose/MWCNT, and cellulose/GNPs inks were performed on TA DHR-1 Rheometer (40 mm parallel steel plate). The shear rate was set as 0.01 to 100 s^{-1}. UV-vis spectrum was collected on a Shimadzu UV3600 UV–vis spectrometer. Deionized water was used as the reference. Fourier transform infrared (FTIR, Nicolet 6700, USA) and Raman spectroscopy (Aramis, HORIBA JOBIN YVON) were carried out to analyze the intermolecular interactions between cellulose and nanomaterials or between urea and nanomaterials. The mechanical properties of the filament was characterized by an LLY-06 electronic monofilament strength tester (Textile Instruments Laizhou Co., Ltd., China). The stretching velocity was set as 20 mm/min, and the ambient temperature was regulated as 25 °C with humidity of 65%. The mechanical properties of RC/MWCNT film was carried out on a Shimadzu AGS-X tester. The stretching velocity was set as 1 mm/min, and the ambient

temperature was regulated as 25 °C with humidity of 65%. Thermal conductivity of RC, RC/BNNSs filament and RC/MWCNT films were calculated according the equation $\kappa = \alpha \rho C$, where κ, α, ρ, and C respectively correspond to thermal conductivity, thermal diffusivity, density and specific heat capacity. The transient electro-thermal (TET) technique is used for measuring α of the filament according to our previous study.[2] And an LFA 467 analyzer (NETZSCH, Germany) was used to measure α of the RC and RC/MWCNT films as the voltage and pulse width were respectively set to be 250 V and 300 μs. C was determined by differential scanning calorimeter (DSC-25, TA) using sapphire as the standard sample. EMI SE properties of porous RC and RC/GNPs nanocomposites (diameter of 13 mm and thickness of 1-2.5 mm) at the frequency range from 8.2 to 12.4 GHz (X-band) was measured by Agilent N5230 vector network analyzer, which is connected with a coaxial test cell (APC-7 connector). Thermogravimetric analysis (TGA 55, TA, USA) was used to analyze the chemical composition of BNNSs, MWCNT or GNPs after intense mixing treatment.

DFT simulation for calculating the system energy and interaction energy: All the MD simulations were performed using the Forcite module of Materials Studio developed by Accelrys In. The condensed-phase optimized molecular potential for atomistic simulation studies (COMPASS) force field was employed to analyze the intramolecular and intermolecular interaction.[3] During the simulation, the electrostatic interactions were calculated using the Ewald method with accuracy of 0.001 kcal/mol, and the van der Waals (vdW) forces were corrected by atom-based summation method with a cutoff radius of 12.5 A. Initially, Geometry Optimization

was performed respectively to reach the stable status with the convergence tolerance value of 0.001 kcal/mol. Then, the model of BN, Graphene, CNT, urea, cellulose and hydroxide were placed at the center of a simulation box with various combination. Geometry Optimization was performed to reach the stable status with the convergence tolerance value of 0.001 kcal/mol. The interaction energy was then calculated via the following formula:[4]

$$E_{interaction} = E_{total} - (E_1 + E_2 + E_3 + \ldots)$$

where $E_{interaction}$ is the interaction energy, E_{total} is the total energy of the combination of molecular models within the simulation box, and E_x (x=1, 2, 3 …) is the energy of individual molecule.

DFT simulation for charge transfer: Density functional theory calculations were conducted to investigate the charge transfer between urea molecule and different nanomaterials.[5] The electron exchange was described by the Perdew-Burke-Ernzerhof (PBE) function along with a generalized gradient approximation (GGA).[6] The projector augmented wave (PAW) method was used to describe the electron-ion interaction. The kinetic energy cutoff for plane wave was chosen as 400 eV.[7] In all calculations, the convergence criterion for atomic energy was set as 10-4 eV and the convergence criterion for atomic was 0.05 eV/Å. A vacuum space of 20 Å was introduced to eliminate the mutual effect of different configurations. For graphene and boron nitride layers, 4× 4× 1 supercells were built to represent the graphene and boron nitride nanosheets. The Brillouin zones were both sampled by using a 4× 4× 1 k-points grid for graphene and boron nitride. A (4, 4) singled walled carbon nanotube was built to model the

carbon nanotubes in the calculation, and the Brillouin zone was sampled by using a 1× 1× 4 k-points. Charge transfer analysis was performed by utilizing Bader Charge.

2. Supplementary Figures and Tables

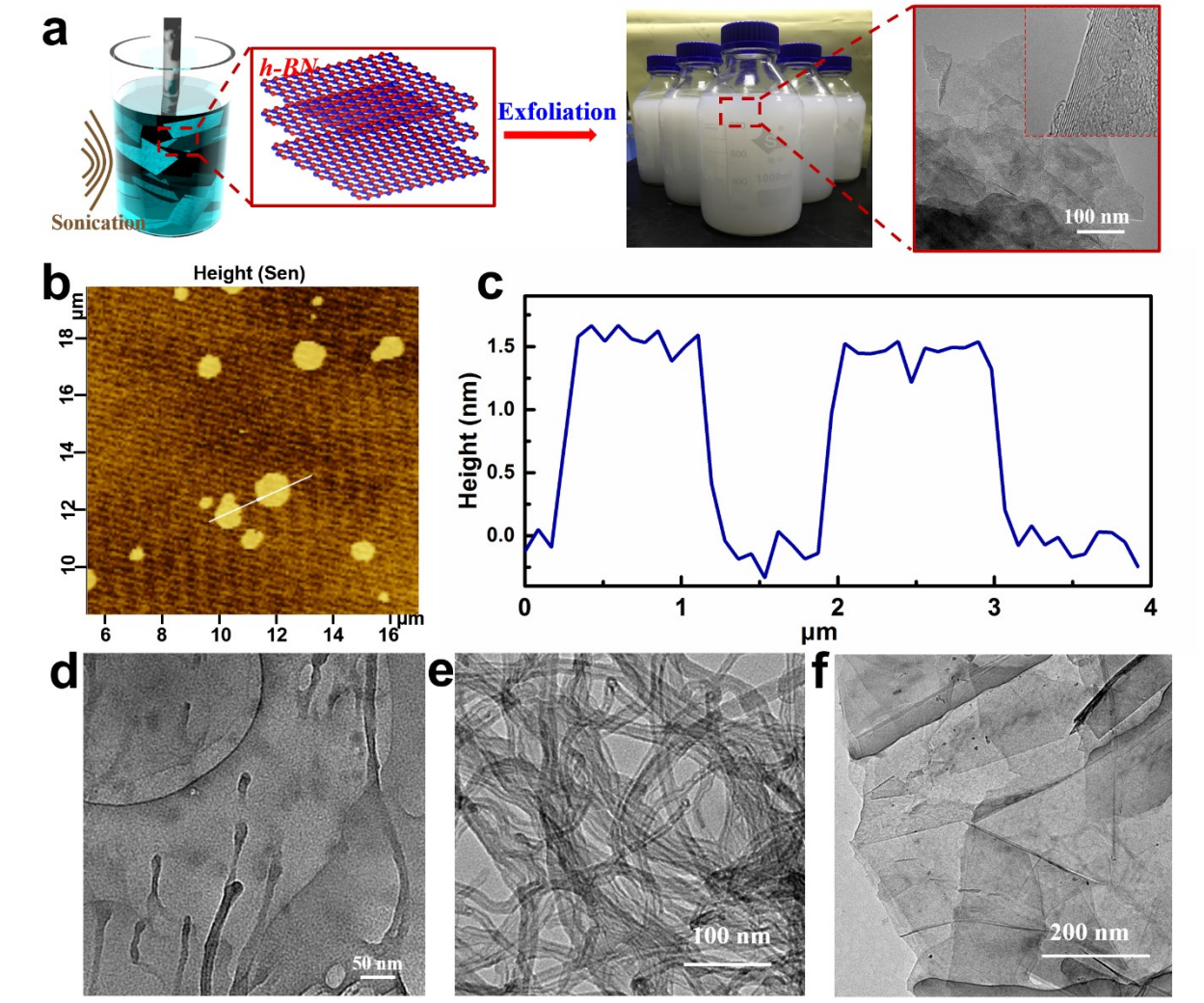

Figure S1. Characterization of nanomaterials. a) Scheme for exfoliation of h-BN, and the optical image with TEM morphology of BNNSs, b) AFM image of BNNSs and c) its corresponding height information, d) worm-like nanocellulose exists in dissolved solution, e) TEM image of MWCNT, f) TEM image of GNPs.

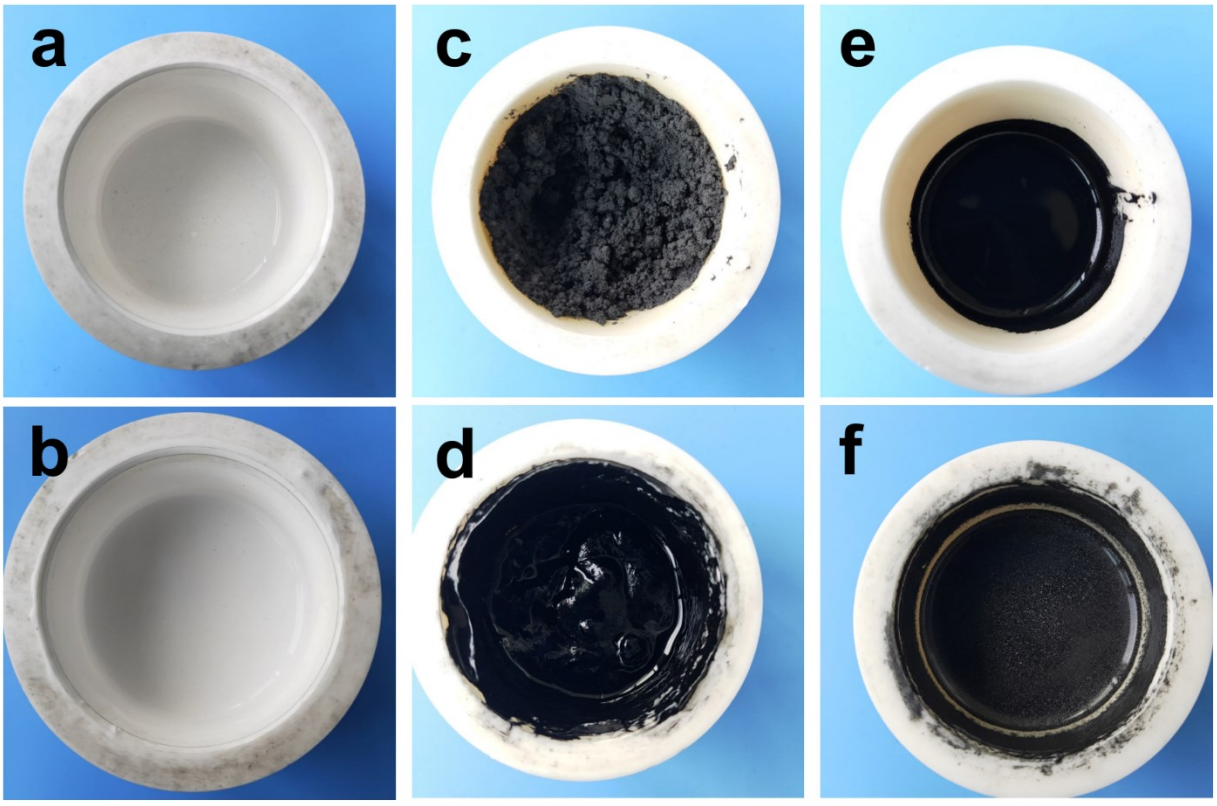

Figure S2. Optical morphology of BNNS/urea aqueous slurry a) before and b) after ball milling, MWCNT/urea aqueous slurry c) before and d) after ball milling, GNPs/urea aqueous slurry e) before and f) after ball milling.

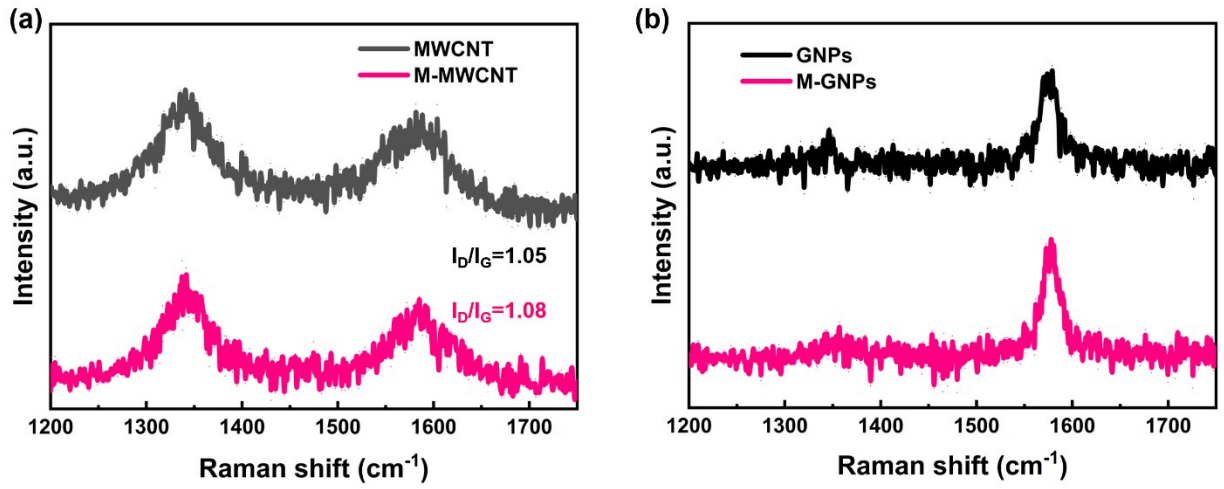

Figure S3. Raman spectra of a) MWCNT and ball-milled MWCNT (M-MWCNT), b) GNPs and ball-milled GNPs (M-GNPs).

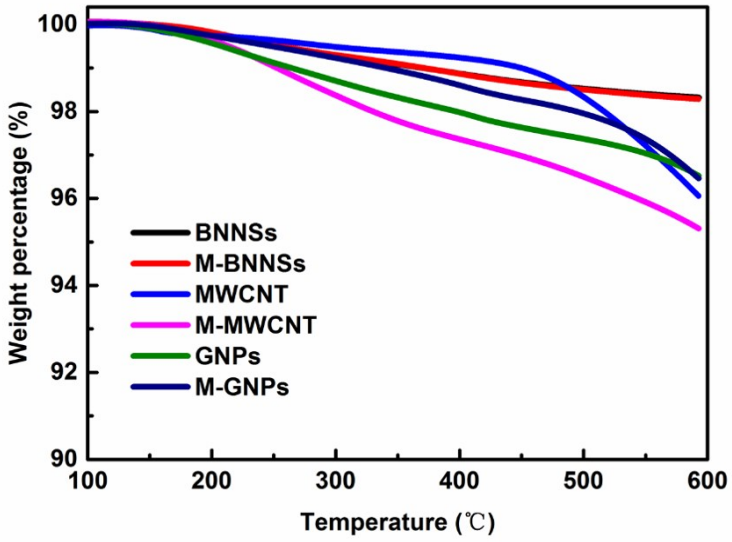

Figure S4. TGA results of BNNSs, ball-milled BNNSs (M-BNNSs), MWCNT, M-MWCNT, GNPs and M-GNPs.

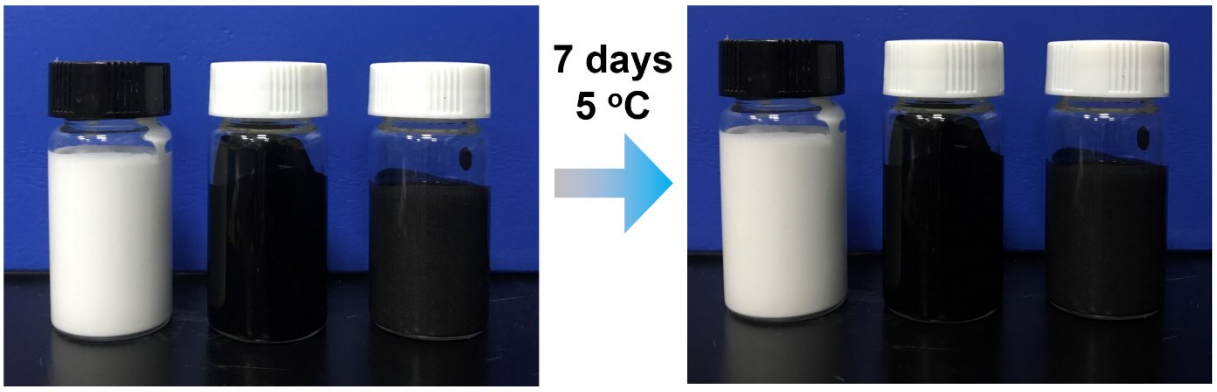

Figure S5. The photographs of cellulose/nanomaterial inks before and after deposited for 7 days at 5 °C. Noted that the samples from left to right are cellulose/BNNSs, cellulose/MWCNT and cellulose/GNPs inks, respectively.

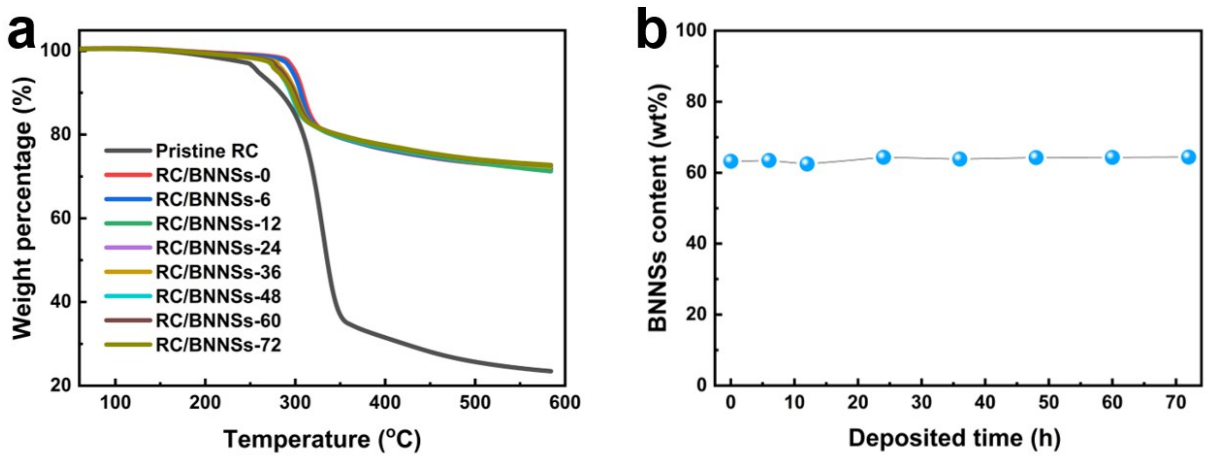

Figure S6. (a) TGA curves of RC or RC composite regenerated from the cellulose/BNNSs hybrids deposited for different times, and (b) their calculated solid BNNSs content as increase of deposited time based on the residual carbon content of pristine cellulose after the same treatment. Noted that RC/BNNSs-x, in which x means the x h cellulose/BNNSs ink has been deposited for.

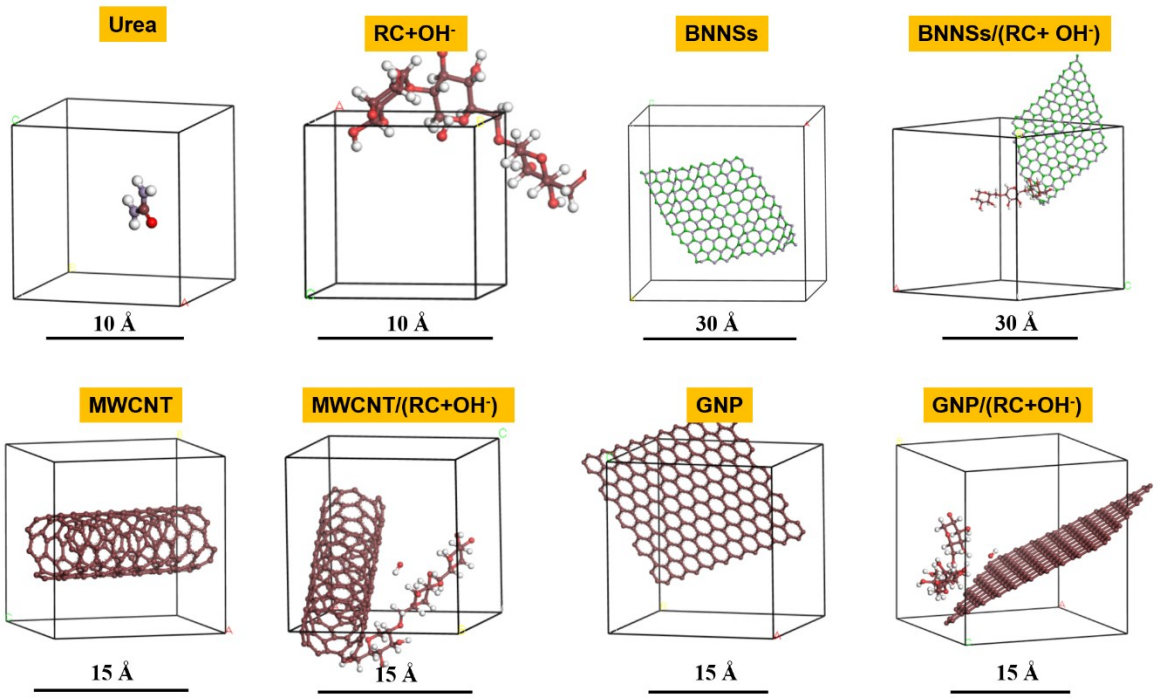

Figure S7. Simulated models for a single nanomaterial, $RC+OH^-$ and their combinations.

Table S1. Calculated total energy of multi-composition systems based on urea and nanomaterial.

Model	BNNSs/Urea	MWCNT/Urea	GNPs/Urea
Energy (kcal/mol)	742.03	1808.31	717.54

Table S2. Calculated interaction energy between ($RC+OH^-$) and nanomaterial.

Model	BNNSs/($RC+OH^-$)	MWCNT/($RC+OH^-$)	GNPs/($RC+OH^-$)
Interaction Energy (kcal/mol)	-81.77	-110.66	-97.81

Table S3. FTIR characteristic peaks of BNNSs, urea, urea/BNNSs and RC/BNNSs.

Peaks (cm^{-1})	B-$N_{stretching}$	B-$N_{bending}$	C=$O_{stretching}$	N-$H_{bending}$	N-$H_{stretching}$
BNNSs	1375.66	818.88	/	/	/
Urea	/	/	1677.1	1622.7	1462.3
Urea/BNNSs	1384.2	802.9	1669	1626	1449.2
RC/BNNSs	1368.7	790.3	/	/	/

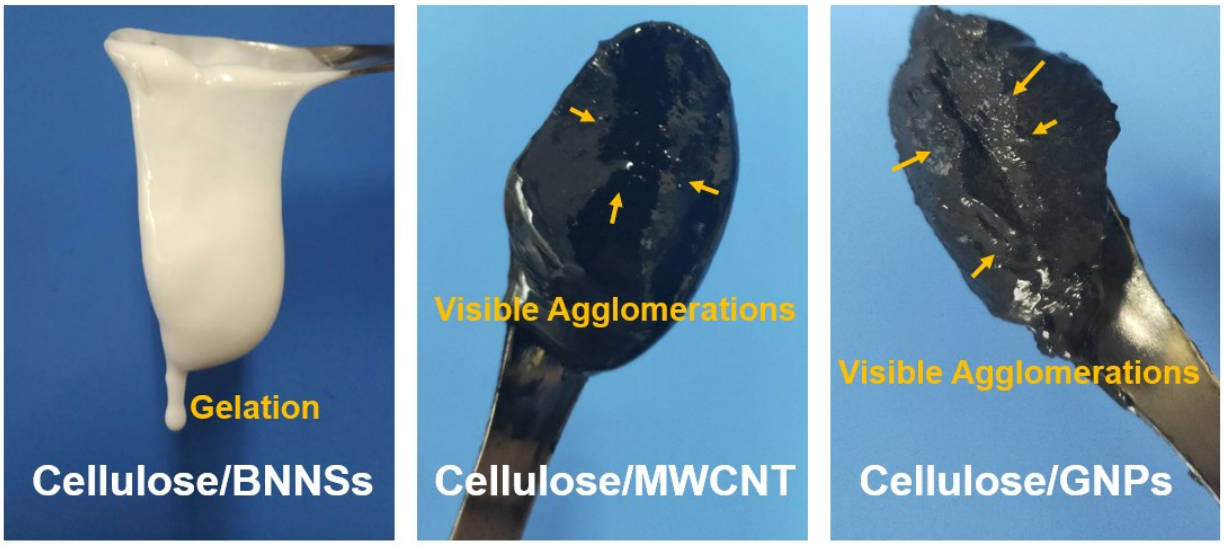

Figure S8. Optical photographs of cellulose/BNNSs ink, cellulose/MWCNT ink and cellulose/GNPs ink via directly mixing cellulose solution and nanomaterial together, without the typical ball-milling treatment.

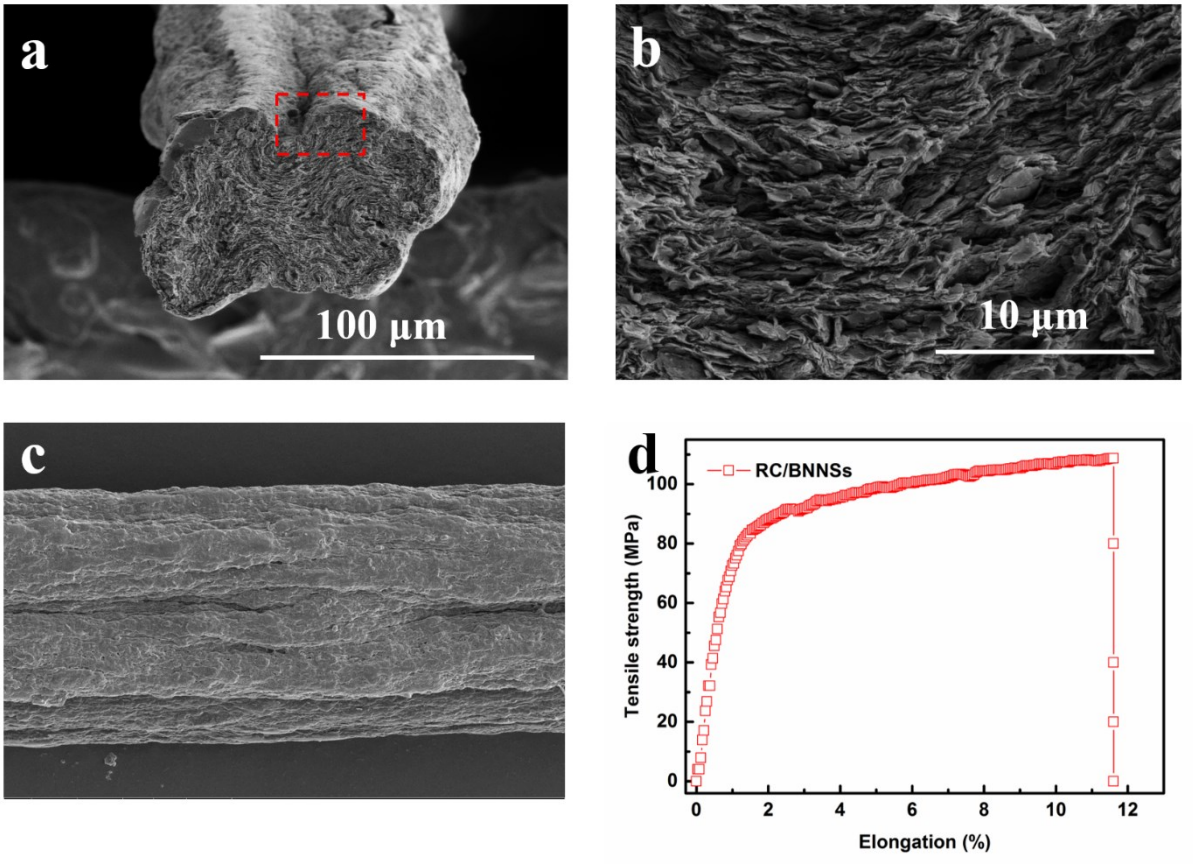

Figure S9. SEM images of fracture surface of RC/BNNSs filament: a) low resolution and b) high resolution, c) SEM image of superficial surface of RC/BNNSs filament, d) tensile strength vs elongation curve of RC/BNNSs filament.

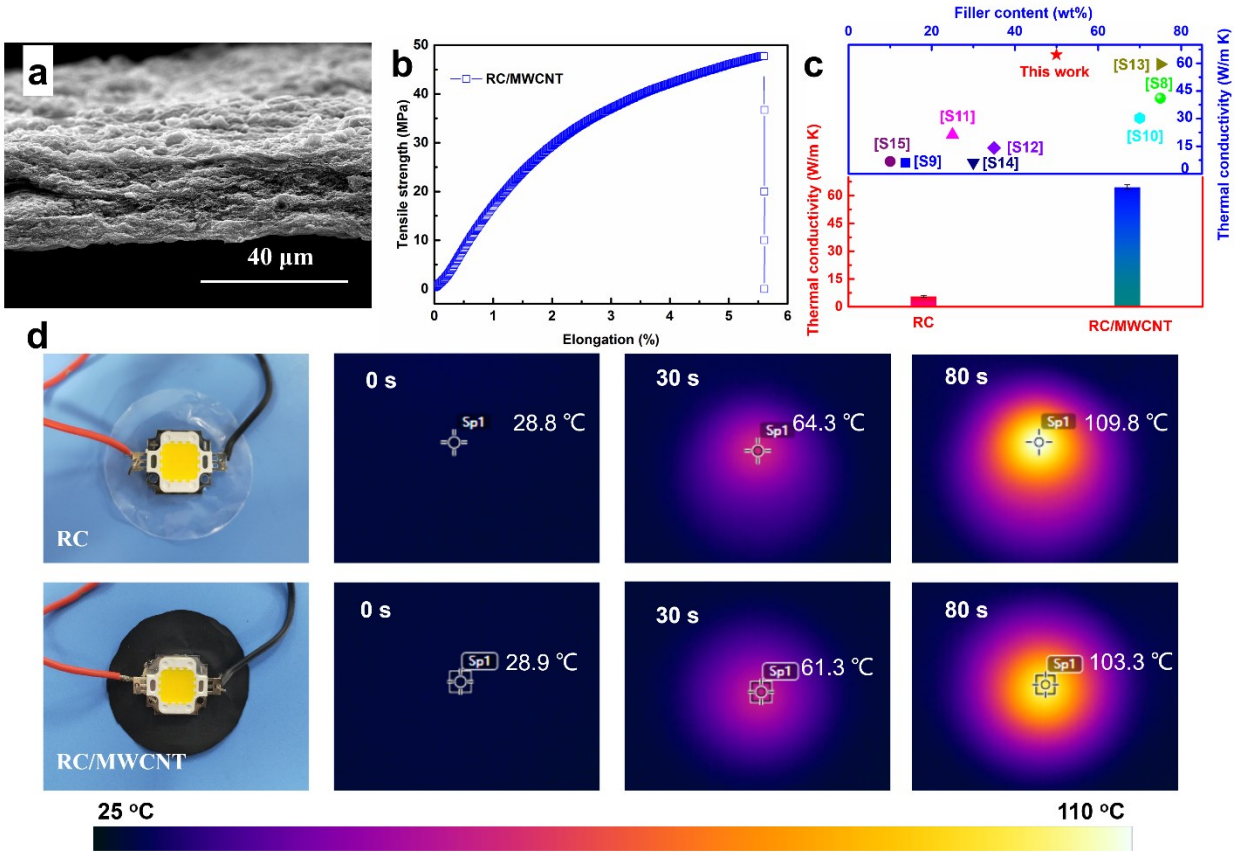

Figure S10. a) SEM image of fracture surface of RC/MWCNT film, b) tensile strength vs elongation of RC/MWCNT film, c) in-plane thermal conductivity of RC/MWCNT film and its comparison with other cellulose-based thermally conductive films,[8-15] d) infrared imaging results exhibit much better thermal management capability of RC/MWCNT film.

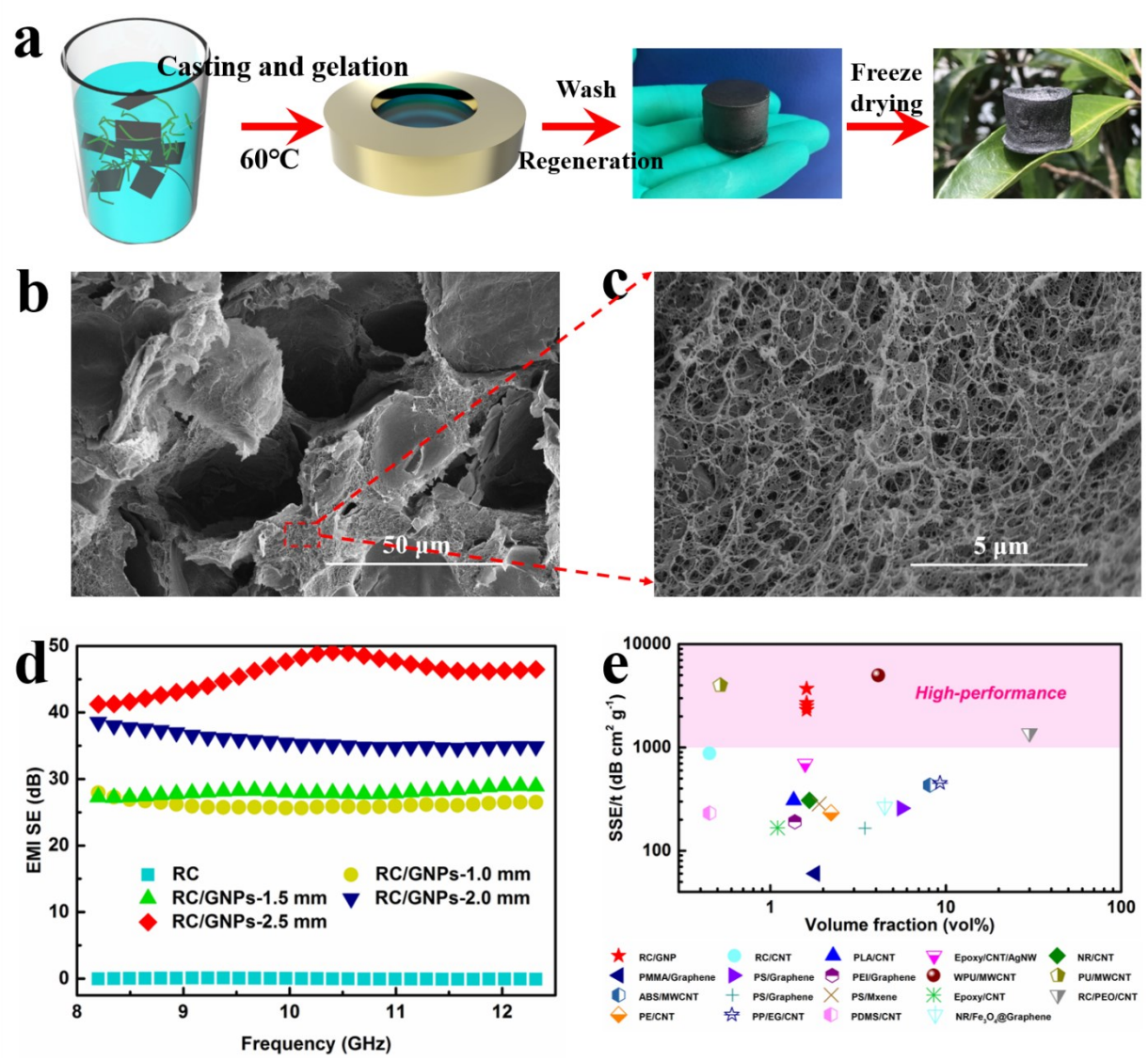

Figure S11. a) Scheme for fabricating 3D porous RC/GNPs foam, SEM images with the b) low resolution and c) low resolution of the RC/GNPs foam, d) X-band electromagnetic interference shielding effectiveness (EMI SE) of RC/GNPs foam with the different thickness, e) specific shielding effectiveness (SSE/t) of RC/GNPs foam and its comparison with previously reported studies.[16-33]

References

1. L. Wu, K. Wu, D. Liu, R. Huang, J. Huo, F. Chen, Q. Fu, *J. Mater. Chem. A* 2018, **6**, 7573-7584.
2. K. Wu, L. Yu, C. Lei, J. Huang, D. Liu, Y. Liu, Y. Xie, F. Chen, Q. Fu, *ACS Appl. Mater. Interfaces* 2019, **11**, 40685-40693.
3. H. Sun, *J. Phys. Chem. B* 1998, **102**, 7338-7364.
4. B. Yu, S. Fu, Z. Wu, H. Bai, N. Ning, Q. Fu, *Composites, Part A* 2015, **73**, 155-165.
5. P.E. Blöchl, *Rev. B* 1994, **50**, 17953.
6. M. C. Payne, M. P. Teter, D. C. Allan, T. Arias, a. J. Joannopoulos, *Rev. Mod. Phys.* 1992, **64**, 1045.
7. W. Kong, F. Gong, Q. Zhou, G. Yu, L. Ji, X. Sun, A. M. Asiri, T. Wang, Y. Luo, Y. Xu, *J. Mater. Chem. A* 2019, **7**, 18823-18827.
8. F. Wang, L. T. Drzal, Y. Qin, Z. Huang, *Composites, Part B* 2015, **79**, 521.
9. Z. Shen, J. Feng, *ACS Appl. Mater. Interfaces* 2018, **10**, 24193.
10. K. Wu, J. Fang, J. Ma, R. Huang, S. Chai, F. Chen, Q. Fu, *ACS Appl. Mater. Interfaces* 2017, **9**, 30035.
11. X. Zeng, J. Sun, Y. Yao, R. Sun, J.-B. Xu, C.-P. Wong, *ACS Nano* 2017, **11**, 5167.
12. X. Wang, P. Wu, *ACS Appl. Mater. Interfaces* 2018, **10**, 34311.
13. G. Li, X. Tian, X. Xu, C. Zhou, J. Wu, Q. Li, L. Zhang, F. Yang, Y. Li, *Compos. Sci. Technol.* 2017, **138**, 179.
14. N. Song, D. Jiao, P. Ding, S. Cui, S. Tang, L. Shi, *J. Mater. Chem. C* 2016, **4**, 305.

15. Y. Yao, X. Zeng, G. Pan, J. Sun, J. Hu, Y. Huang, R. Sun, J.-B. Xu, C.-P. Wong, *ACS Appl. Mater. Interfaces* 2016, **8**, 31248.

16. Q. Zhang, Q. Liang, Z. Zhang, Z. Kang, Q. Liao, Y. Ding, M. Ma, F. Gao, X. Zhao, Y. Zhang, *Adv. Funct. Mater.* 2018, **28**, 1703801.

17. H.-D. Huang, C.-Y. Liu, D. Zhou, X. Jiang, G.-J. Zhong, D.-X. Yan, Z.-M. Li, *J. Mater. Chem. A* 2015, **3**, 4983.

18. T. Kuang, L. Chang, F. Chen, Y. Sheng, D. Fu, X. Peng, *Carbon* 2016, **105**, 305.

19. Y. Xu, Y. Li, W. Hua, A. Zhang, J. Bao, *ACS Appl. Mater. Interfaces* 2016, **8**, 24131.

20. Y. Zhan, M. Oliviero, J. Wang, A. Sorrentino, G. G. Buonocore, L. Sorrentino, M. Lavorgna, H. Xia, S. Iannaced, *Nanoscale* 2019, **11**, 1011.

21. H.-B. Zhang, Q. Yan, W.-G. Zheng, Z. He, Z.-Z. Yu, *ACS Appl. Mater. Interfaces* 2011, **3**, 918.

22. D.-X. Yan, P.-G. Ren, H. Pang, Q. Fu, M.-B. Yang, Z.-M. Li, *J. Mater. Chem.* 2012, **22**, 18772.

23. J. Ling, W. Zhai, W. Feng, B. Shen, J. Zhang, W. G. Zheng, *ACS Appl. Mater. Interfaces* 2013, **5**, 2677.

24. Z. Zeng, H. Jin, M. Chen, W. Li, L. Zhou, Z. Zhang, *Adv. Funct. Mater.* 2016, **26**, 303.

25. M. H. Al-Saleh, W. H. Saadeh, U. Sundararaj, *Carbon* 2013, **60**, 146.

26. D. X. Yan, H. Pang, B. Li, R. Vajtai, L. Xu, P. G. Ren, J.-H. Wang, Z.-M. Li, *Adv. Funct. Mater.* 2015, **25**, 559.

27. R. Sun, H. B. Zhang, J. Liu, X. Xie, R. Yang, Y. Li, S. Hong, Z.-Z. Yu, *Adv. Funct. Mater.* 2017, **27**, 1702807.

28. Y. Chen, H. B. Zhang, Y. Yang, M. Wang, A. Cao, Z. Z. Yu, *Adv. Funct. Mater.* 2016, **26**, 447.

29. L.-Q. Zhang, B. Yang, J. Teng, J. Lei, D.-X. Yan, G.-J. Zhong, Z.-M. Li, *J. Mater. Chem. C* 2017, **5**, 3130.

30. L.-C. Jia, D.-X. Yan, C.-H. Cui, X. Jiang, X. Ji, Z.-M. Li, *J. Mater. Chem. C* 2015, **3**, 9369.

31. K. Wu, Y. Xue, W. Yang, S. Chai, F. Chen, Q. Fu, *Compos. Sci. Technol.* 2016, **130**, 28.

32. D. Lu, Z. Mo, B. Liang, L. Yang, Z. He, H. Zhu, Z. Tang, X. Gui, *Carbon* 2018, **133**, 457.